Study of the optimal active control of a trombone

Colas Cavaillès, Bruno Gazengel, Manuel Melon, Christophe Ayrault

Acta Acustica 2022, **6**, 18
© The Author(s), Published by EDP Sciences, 2022
https://doi.org/10.1051/aacus/2022015

Available online at:
https://acta-acustica.edpsciences.org

SCIENTIFIC ARTICLE OPEN ACCESS

Study of the optimal active control of a trombone

Colas Cavaillès*, Bruno Gazengel, Manuel Melon, and Christophe Ayrault

Laboratoire d'Acoustique de l'Université du Mans (LAUM), UMR 6613, Institut d'Acoustique - Graduate School (IA-GS), CNRS, Le Mans Université, 72085 Le Mans Cedex 9, France

Received 12 January 2022, Accepted 31 March 2022

Abstract – In the brass instrument family, the sound can be modified or attenuated using a mute, which is usually inserted in the bell of the instrument. The objective of this paper is to study the principle and the technological feasibility of an active mute using loudspeakers placed in front or around the instrument bell. This mute must reduce the acoustic power emitted by the instrument while avoiding any impact on its playability. At this stage, an optimal control is considered and no real-time controller is implemented. Results show that an active control placed outside the trombone is theoretically feasible and can be efficient to reduce the acoustic power up to 2000 Hz by placing a ring of sources around the bell and a source in front of the trombone. The instrument input impedance is very slightly affected by the control. In accordance with numerical simulations, the experiment showed that placing a control speaker very close in front of the bell of the instrument modifies the pressure field of the instrument in such a way that it allows to obtain a power attenuation greater than the predicted one. The control is technologically achievable but requires a high power for the closest source.

Keywords: Musical Acoustics, Electroacoustics, Active Control, Brass instruments, Transducers

1 Introduction

The sound rendering of a musical instrument is essential for the musician who must be able to vary the sound level as well as the timbre of its instrument as he wishes. In the brass family, the sound can be modified or attenuated using a mute, which is usually inserted in the bell of the instrument or placed near it. This device, existing in various shapes, has an impact on both the timbre and the power of the radiated sound [1]. Musicians mainly use it to produce sound effects such as the "wah-wah" effect [2]. It can also be a way to reduce the radiated sound level with a practice mute so that one can play without disturbing the neighborhood.

A common impact of the mutes is the inevitable modification of the instrument input impedance which alters the musician's playing. For instance a dry mute shifts the input impedance peaks towards high frequencies [2–5]. New resonance peaks also appear when a mute is inserted, in particular an extra impedance peak between the first and second resonance, which seems to make it more difficult to play any note having a fundamental frequency close to this peak [6, 7]. The impedance of the instrument is thus altered and the musician must therefore adapt his way of playing. In 1995, Yamaha developed the SILENT Brass Mute[1], which allows to play a brass instrument while enclosing the acoustic energy inside the instrument. The sound is picked up by a microphone in the mute and then transmitted through headphones to the player's ears.

In 1998, Pickett tried to perform active control on a trumpet [8] putting the control source inside the bell. The microphone was placed in the mouthpiece, which essentially picked up the sound of the trumpet and rejected any interference. A control is thus possible but only theoretically. The technological limitation of this work is the capacity of the loudspeaker to generate a source strength that can control the propagating wave inside the trumpet and which must be simultaneously small and light.

An optimal active control on an endblown flute was investigated in 1998 [9]. Several small microphones were placed in the cylindrical tube allowing to measure incoming and reflected waves from the front and the back. A signal sent to the control speaker was used to cancel the reflected wave.

A study on active control for a trombone was carried out by Meurisse *et al.* [7]. A feedback control allowed to suppress the extra impedance peak due to the mute between the two first peaks in the input impedance of the trombone. A modal control was also studied in the context of active control of the clarinet [10]: the control source located inside the instrument allowed significant changes of the sound and input impedance of the instrument. It allowed to modify the playability and the sound of the instrument.

*Corresponding author: colas.cavailles@univ-lemans.fr

[1] Yamaha – SILENT Brass™ Series – www.yamaha.com/en/about/design/synapses/id_061 (2022).

A gong with geometric nonlinearities was studied experimentally in [11]. The control allowed to change the damping of the fundamental mode of the structure. The damping control provided good results for small amplitude regime once the instantaneous frequency of the mode reaches a stabilized frequency range.

Buys *et al.* attempted to create a hybrid wind instrument by using a loudspeaker to excite a clarinet-type tube [12]. The reed-beating pressure and the oscillation thresholds were estimated and appeared to be nearly the same in both the hybrid and simulated situation. The interaction between the speaker and the tube was compensated by a feedback filter while the loudspeaker response was corrected by a feedforward filter.

In 2016, Ayrault *et al.* conducted a study on the effect of an active control on the outer waveguide radiation [13]. The objective was to reduce the radiated power by an active control with two secondary sources located outside the instrument. This theoretical study showed that the directivity can also be modified by adding a time delay to the control sources. This however strongly reduces the desired power attenuation. In this case, the active mute has a significant impact on the radiated sound but a rather slight influence on the input impedance of the instrument by shifting the peak by about ten cents towards the high frequencies. The work presented below is based on this paper and studies a trombone as the source to control.

More recently, Ayrault *et al.* investigated an active mute mounted in the bell of a simplified trumpet (cylindrical tube connected to an exponential bell) [14]. Up to six speakers can be mounted on the mute. Different models have been studied to predict the input impedance and the pressure radiated by the instrument during an optimal active control. When the objective of the control is to increase the radiated sound level, the amplitude of the impedance peaks is modified.

The trombone can radiate a high sound level up to 110 dB SPL at 1 m in free field. In terms of radiation, the instrument can be assimilated to a monopole in low frequencies – up to 500 Hz [15].

Knowing these characteristics, the objective of this paper is to study the principle and technological feasibility of an active mute using secondary sources (loudspeakers) placed in front or around the instrument bell. This mute must reduce the acoustic power emitted by the instrument while limiting its impact on the playability of the musical instrument. At this stage, an optimal control is considered and no real-time controller is implemented.

The studied system is first presented in Section 2 before developing the theory underlying the different active control strategies. Section 3 is dedicated to the assessment of the different control strategies performances. The acoustic power control is evaluated using measurements performed in an anechoic chamber in Section 4. The effect of the control on the instrument input impedance is then carried out to assess whether the control can have an impact on the musician's playing. In Section 5, the trombone volume velocity is estimated in order to precisely characterize the primary source to be controlled. Finally the paper deals with technological limits of the loudspeakers used as secondary sources in order to propose a system which can be used for real musical applications.

2 Theory

This section presents the system under study and the theoretical aspects of the control. It shows how to estimate the optimal secondary source strengths which enable to minimize the radiated power.

2.1 System under study

The system under study is a trombone equipped with N_s control loudspeakers placed near the bell. The pressure radiated by the sources is measured with M receivers. Figure 1 shows an example including the primary source s_0 (equivalent source of the instrument), 6 secondary sources s_1 to s_6 and one receiver r_1. On this example, each control source is separated from the primary one by the same distance h as all the control sources are placed on a ring. More generally, the control sources can be placed anywhere near the bell. An example of the experimental setup is presented in Figure 5 for a plastic trombone.[2]

The optimal control consists in applying an optimal control filter:

$$\boldsymbol{w} = \frac{\boldsymbol{x}_s^{\mathbf{opt}}}{x_0}, \tag{1}$$

where x_0 is the reference signal describing the primary source (volume velocity or voltage, depending on the approach) and $\boldsymbol{x}_\mathbf{s}^{\mathbf{opt}}$ is the driving signal of the secondary sources (volume velocity or voltage) which aim is to reduce the primary source power.

Depending on the configuration, the optimal filter $\boldsymbol{w}$ is estimated as follows:

- the active control theory is first developed with all the sources considered as simple monopoles, then: $\boldsymbol{w_1} = \frac{\boldsymbol{q}_s^{\mathbf{opt}}}{q_0}$ where q_0 is the primary source volume velocity. The transfer impedance matrix between sources permits to estimate the theoretical optimal source strengths $\boldsymbol{q}_s^{\mathbf{opt}} = [q_1^{\text{opt}}(\omega), q_1^{\text{opt}}(\omega), \cdots, q_N^{\text{opt}}(\omega)]^T$ in an analytical way as described in [16]. This approach called the "near field control" is used later to optimize the number and positions of secondary sources in Section 3.
- In Section 4, real sources (trombone excited by a compression driver as the primary source and control loudspeakers as secondary sources) are considered for an experimental setup with the control filter: $\boldsymbol{w_2} = \frac{\boldsymbol{u}_s^{\mathbf{opt}}}{u_0}$ where u_0 is the excitation voltage of the compression driver placed at the trombone input. Knowing the primary pressure radiated in far field, the optimal secondary voltage vector $\boldsymbol{u}_s^{\mathbf{opt}}$ is estimated from the transfer function matrix linking primary

[2] Plastic Trombone pBone – https://www.pbone.co.uk (2022).

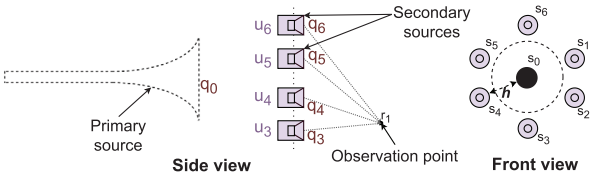

Figure 1. System under study composed of a trombone considered as the primary source of volume velocity q_0, N_s loudspeakers considered as secondary sources of volume velocity $\boldsymbol{q_s}$, due to voltage inputs $\boldsymbol{u_s}$ and $\boldsymbol{M}$ receivers ($N_s = 6$, $M = 1$ in this figure).

and secondary sources voltage and receivers pressure. A cost function is written to minimize the acoustic power with [17, 18]. This approach is called "far field control".

- The last configuration consists in a trombone played by a musician. In this case, the volume velocity of the trombone q_0 is estimated from the measurement of the pressure radiated by the instrument (see Sect. 5). This enables to deduce the optimal filter $\boldsymbol{w_3} = \frac{\boldsymbol{u_s^{opt}}}{q_0}$ as presented in Section 2.2.3.

2.2 Power minimization

2.2.1 Near field control

In this section, the system is assumed to be composed of $N_s + 1$ ideal sources (monopoles). The volume velocity vector $\boldsymbol{q}$ is defined by $\boldsymbol{q} = [q_0(\omega), q_1(\omega), \cdots, q_N(\omega)]^T$ where $q_n(\omega)$ is the strength of the source n, with $n = 0$ for the primary source and $n = 1 \rightarrow N_s$ for the secondary sources. The radiated pressure is written $\boldsymbol{p} = [p_1, p_2, \cdots, p_{\mathrm{M}}]^T$.

Nelson *et al.* [16] show that the optimal source strength to be applied to the secondary source minimizing the primary source power can be written:

$$\boldsymbol{q_s^{opt}} = -\mathbf{A_0}^{-1}\mathbf{b_0}, \tag{2}$$

with $\boldsymbol{A_0} = \frac{1}{2}\Re\{\mathbf{Z_{ss}}\}$, $\boldsymbol{b_0} = \frac{1}{2}\Re\{\boldsymbol{z_{0s}}\}q_0$, where $\Re$ denotes the real part operator, $\boldsymbol{Z_{ss}}$ the transfer impedance matrix between each secondary source and $\boldsymbol{z_{0s}}$ the transfer impedance vector between the primary source and each secondary source, both being defined by $\boldsymbol{p} = \boldsymbol{Zq}$ where $\boldsymbol{Z}$ is the transfer impedance matrix such as:

$$Z_{ij} = jk\rho c\frac{\mathrm{e}^{-jkr_{ij}}}{4\pi r_{ij}}, \tag{3}$$

with k the wavenumber, ρ the air density, c the celerity of sound and r_{ij} the distance between sources i and j. In a case where regularization in the matrix $\boldsymbol{A_0}$ is added [23], it comes:

$$\boldsymbol{A_0} = \frac{1}{2}\Re\{\boldsymbol{Z_{ss}}\} + \beta\boldsymbol{I}, \tag{4}$$

with β the regularization factor. $\beta = 0$ to get $\boldsymbol{A_0}$ without regularization and $\boldsymbol{I}$ an identity matrix.

2.2.2 Far field control

A real trombone and real secondary sources (loudspeakers) are considered in this section. As the impedance transfer matrix $\boldsymbol{Z}$ between each source defined with equation (3) cannot be measured easily in practice (due to the difficulty of measuring the volume velocity), transfer functions between the pressure in far field and source excitation voltage are measured.

The primary source pressure $\boldsymbol{p_0} = [p_{01}, p_{02}, \cdots, p_{0M}]^T$ is given by:

$$\boldsymbol{p_0} = \boldsymbol{g_0}q_0, \tag{5}$$

where the transfer impedance vector for the primary source $\boldsymbol{g_0}$ is estimated by $g_0(i) = \frac{jk\rho c e^{-jkr(i)}}{4\pi r(i)}$. The pressure produced by the secondary sources $\boldsymbol{p_s} = [p_{\mathrm{s}1}, p_{\mathrm{s}2}, \cdots, p_{\mathrm{s}M}]^T$ is given by $\boldsymbol{p_s} = \boldsymbol{G_s}\boldsymbol{q_s}$ with $\boldsymbol{q_s}$ the volume velocity of the secondary sources and $\boldsymbol{G_s}$ the transfer impedance matrix for the secondary sources. As q_0 can not be measured easily in a direct manner and in order to manage the primary source excitation, the trombone is modified and is excited by a compression driver through an adaptation tube (presented in Sect. 4.1). The pressure radiated by this adapted trombone is written $\boldsymbol{p_0} = \boldsymbol{h_0}u_0$ where $\boldsymbol{h_0}$ is the transfer function vector.

The secondary source pressure is written $\boldsymbol{p_s} = \boldsymbol{H_s}\boldsymbol{u_s}$ with $\boldsymbol{u_s}$ the secondary source voltage vector (with N_{s} secondary sources) and $\boldsymbol{H_s}$ the transfer function matrix between source voltages and microphone pressures (size $M \times N_{\mathrm{s}}$).

The objective is to find the secondary source optimal voltages $\boldsymbol{u_s^{opt}}$ as a function of the primary source voltage u_0 minimizing a cost function. As the objective is to minimize the power radiated by the system, the power W is estimated from the pressure measured with M microphones placed in far field on a sphere of radius r with constant angle steps $\Delta\theta$ for the azimuth angle and $\Delta\phi$ for the elevation angle. The total power W – including the power of the primary source W_0, of the secondary sources W_{s} and of the interferences created between sources W_l [19, 20] – is expressed as the sum of the quadratic pressures at the receivers $\boldsymbol{r}$ defined by the spherical coordinates $\boldsymbol{r} = (r, \theta, \phi)$ as:

$$W = \int_0^{2\pi}\int_0^{\pi}\frac{|p(\boldsymbol{r})|^2}{2Z_c}\mathbf{d}\boldsymbol{S}, \tag{6}$$

with Z_c the characteristic impedance, $p(\boldsymbol{r})$ the superposition of the primary and the secondary sources pressure written as:

$$p(\boldsymbol{r}) = p_0(\boldsymbol{r}) + \sum_{i=1}^{N_{\mathrm{s}}} p_i(\boldsymbol{r}), \tag{7}$$

and $\mathbf{d}\boldsymbol{S}$ the variable surface element written as:

$$\mathbf{d}\boldsymbol{S} = r^2\mathbf{sin}(\boldsymbol{\theta})\mathrm{d}\theta\mathrm{d}\phi. \tag{8}$$

For M microphones placed on a sphere of radius r with constant $\Delta\theta$ and $\Delta\phi$, a discrete approximation of Equation (6) is given by:

$$W \simeq r^2 \Delta\theta \Delta\phi (\boldsymbol{s}[\boldsymbol{p_0} + \boldsymbol{p}_s])^H (\boldsymbol{s}[\boldsymbol{p_0} + \boldsymbol{p}_s]), \quad (9)$$

where the superscript "H" is the Hermitian transpose of a vector and $\boldsymbol{s}$ is a $\boldsymbol{M} \times \boldsymbol{M}$ matrix defined by $s_{ij} = \sqrt{|\sin(\theta_i)|}\delta_{ij}$ with an identity matrix δ_{ij}. The functional to be minimized becomes:

$$J_1 = (\boldsymbol{s}[\boldsymbol{p_0} + \boldsymbol{p}_s])^H (\boldsymbol{s}[\boldsymbol{p_0} + \boldsymbol{p}_s]), \quad (10)$$

to finally take the following form:

$$J_1 = \boldsymbol{u}_s^H \boldsymbol{A_1} \boldsymbol{u}_s + \boldsymbol{u}_s^H \boldsymbol{b_1} + \boldsymbol{b_1}^H \boldsymbol{u}_s + c_1, \quad (11)$$

with the matrix $\boldsymbol{A_1} = \boldsymbol{H}_s^H \boldsymbol{S} \boldsymbol{H}_s$ with $\boldsymbol{S}$ a $\boldsymbol{M} \times \boldsymbol{M}$ matrix defined by $S_{ij} = |\sin(\theta_i)|\delta_{ij}$, the vector $\boldsymbol{b_1} = \boldsymbol{H}_s^H \mathbf{Sh_0} u_0$ and the scalar $c_1 = u_0^* \boldsymbol{h_0}^H \mathbf{Sh_0} u_0$, u_0^* being the complex conjugate of u_0.

To minimize the power W, the optimal secondary voltage to be applied comes from the quadratic function developed by equation (11) and knows a unique solution given by:

$$\boldsymbol{u}_s^{\mathbf{opt}} = -\boldsymbol{A}_1^{-1} \boldsymbol{b_1}. \quad (12)$$

2.2.3 Application to a trombone played by a musician

When the instrument is played by a trombone player, the optimal filter $\boldsymbol{w_3} = \frac{\boldsymbol{u}_s^{\mathbf{opt}}}{q_0}$ needs to be known and the volume velocity q_0 must be measured to deduce $\boldsymbol{u}_s^{\mathbf{opt}}$. Filter $\boldsymbol{w_3}$ is deduced from the results of the previous Section 2.2.2. Writing that:

$$\boldsymbol{w_3} = \frac{\boldsymbol{u}_s^{\mathbf{opt}}}{u_0} \frac{u_0}{q_0}, \quad (13)$$

for a compression driver replacing the trombonist, the problem is to estimate the $\frac{u_0}{q_0}$ when the trombone is excited by a loudspeaker.

Assuming that the primary source is a monopole and its position is known, $\frac{u_0}{q_0}$ is estimated by $\frac{u_0}{q_0} = \frac{u_0}{\boldsymbol{p_0}} \frac{\boldsymbol{p_0}}{q_0} = \boldsymbol{h}_0^+ \boldsymbol{g_0}$ and r the distance from the bell of the trombone to the observation point. This leads to:

$$\boldsymbol{w_3} = \frac{\boldsymbol{u}_s^{\mathbf{opt}}}{u_0} \boldsymbol{h}_0^+ \boldsymbol{g_0}, \quad (14)$$

here $\boldsymbol{h}_0^+ = [\boldsymbol{h}_0^H \boldsymbol{h_0}]^{-1} \boldsymbol{h}_0^H$ is the pseudo-inverse (superscript "+") of $\boldsymbol{h_0}$.

3 Simulation with point sources

In this section, primary and secondary sources are limited to monopoles [16] as presented in Section 2.2.1 and the optimal volume velocity is given by equation (2). This enables to choose the position and the number of secondary sources that will be used in the following in order to optimize the power attenuation:

$$\mathrm{Att}_W = 10 \log_{10} \frac{W_0}{W_{\mathrm{tot}}}, \quad (15)$$

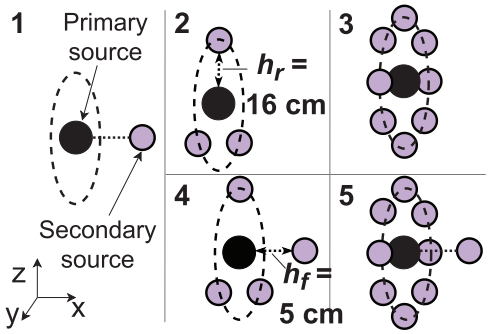

Figure 2. Five configurations for active control: the secondary sources are positioned around the primary source either on a ring at $h_r = 0.16$ m or either in front of this last one at $h_f = 0.05$ m. Vector $\boldsymbol{h}$ gathers the distances between each secondary source and the primary one.

with the primary source power W_0 and the total power W_{tot}, both calculated from the pressure estimated numerically with equation (6). Five secondary source configurations are investigated and shown in Figure 2. The position of these sources is given by vector $\boldsymbol{h}$ gathering each distance between the primary and the secondary sources. $\boldsymbol{h}$ was chosen for practical reasons during the experiment presented in Section 4. The distance $h_r = 0.16$ m allows to place the loudspeakers on the same plane around the bell of the trombone on a ring whose radius is 0.105 m while the distance $h_f = 0.05$ m is chosen to place a control loudspeaker close to the bell in front of the trombone without obstructing the waveguide.

The power attenuation for each case is shown in Figure 3 which illustrates that increasing the secondary sources number (from 3 to 8 sources – cases **2** and **3**) generates almost the same attenuation in the low frequency range. As shown in [21], the power attenuation almost no further increases beyond 4 monopoles equally distributed around the primary source. This explains why there isn't improvement in low frequency between cases **2** and **3** – simulating respectively 3 and 8 secondary sources equally distributed around the primary one. Case **3** (8 sources) allows nevertheless to reduce the needed volume velocity to apply to each source as shown in Figure 4a. Configuration **3** also provides a little more attenuation Att_W above $kh = n\pi$ ($f \simeq 1000$ Hz) but this increase is not sufficient in view of the added system complexity.

When there is only one secondary source, $q_1 = -q_0$ in low frequency whereas with N_s control sources, the required volume velocity is divided by the number of sources. In higher frequencies, q_1 decreases as the power attenuation Att_W drops to 0 for $kh = n\pi$.

For particular cases where secondary sources are not equally distributed around the primary one, the matrix inversion favors the secondary sources placed on the ring at low frequencies (cases **4** and **5**). Due to a very high conditioning at low frequencies bringing singular values to the matrix, the volume velocity required by the secondary source placed in front of the source is thus almost zero in this frequency band. For a theoretical study on

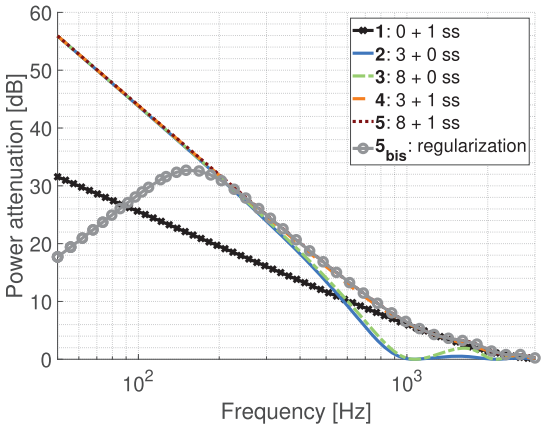

Figure 3. Power attenuation Att_W with a monopole model for the 5 cases presented in Figure 2. Effect of regularization ($\beta = 200$) is shown on the solid curve with circles for case **5**.

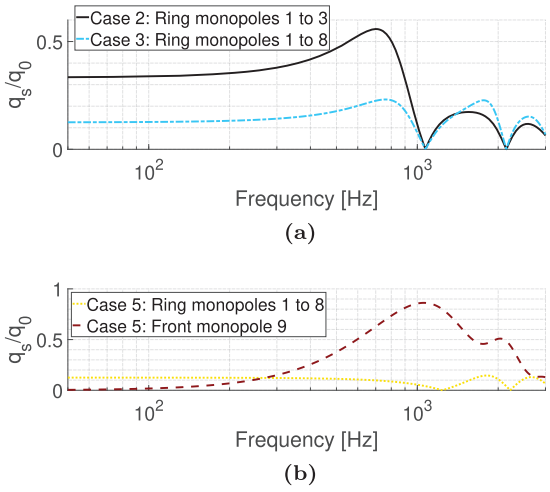

Figure 4. Volume velocity ratio $\frac{q_s}{q_0}$ with a monopole model for various cases presented in Figure 2. (a): the solid line represents each of the 3 secondary sources of the case **2** while the dashed and dotted one represents each of the 8 secondary sources for the case **3**. (b): the dashed line represents the secondary source placed in front of the primary one and the dotted line represents each of the 8 secondary sources placed on the ring, both for case **5** without and with (same curves with circles) regularization with $\beta = 200$.

the feasibility of control, it is thus necessary to regularize $\boldsymbol{A_0}$ before doing the matrix inversion as mentioned by [22, 23]: "the use of regularization function is effective in restoring the strength of acoustic sources when the inverse problem is badly conditioned". Result is shown for case **5** without and with regularization ($\beta = 200$) in Figure 4b.

The addition of a secondary source closer to the primary source (cases **4** and **5**) raises Att_W around $kh = n\pi$ up to 6 dB, allowing a better power attenuation. It is interesting to see that for these two cases, the closer secondary source must provide a larger volume velocity as shown in Figure 4b.

This study is however carried out for an ideal case with point sources, which does not represent the trombone radiation at medium and high frequencies.

4 Experiment

The system is now studied experimentally in order to compare theoretical and measured attenuations due to the control and to evaluate its impact on the input impedance. The aim is to take into account the measured transfer functions between the trombone, the loudspeakers and the receivers (as presented in Sect. 2.2.2) in order to estimate the secondary source optimal voltages $\boldsymbol{u_s^{opt}}$ defined by equation (12).

4.1 Experimental setup

The experiment takes place in the anechoic chamber of the LAUM laboratory. It consists in a trombone (pBone) connected to a 1 m plastic pipe excited with a compression driver *Faital HF10AK* (Figs. 5 and 6). In a first case, 8 control loudspeakers *Beyma 3FR30Nd* are placed around the trombone bell, on a ring of 0.16 m radius whose center corresponds to the trombone's bell one. Another control loudspeaker is placed in front of the bell at $h_f = 0.05$ m for a second setup as in case **5** of Figure 2.

All the loudspeakers are excited with a swept sine between 40 Hz and 3 kHz. This lower frequency limit is

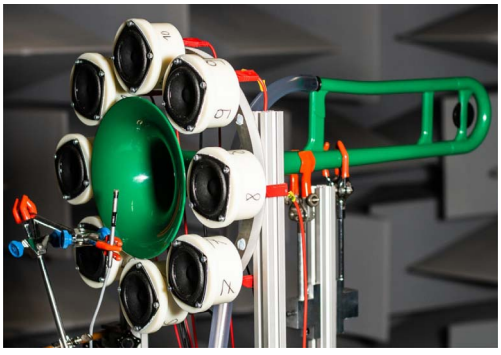

Figure 5. Primary source controlled by eight secondary sources placed on a ring around the bell.

chosen knowing the lowest fundamental frequency played by the trombone (i.e. B♭1, $f_0 = 58$ Hz). The higher frequency is around 3 kHz where the optimal control is not efficient anymore as shown in Figure 3.

Acoustic pressures are measured at 614 points distributed on a sphere of radius $r = 1.94$ m, $\Delta\phi = 9°$ and $\Delta\theta = 10°$ as shown in Figure 6. In practice, only 10 receivers (1/2″ microphones: *B&K 4190* and *GRAS 40-AG*) are positioned on a quarter-circle rod while the trombone and secondary sources are placed on a turntable. This last one is rotated every 10° over 360°. The pressure can thus be measured only on the upper half of the sphere. The trombone and the ring of secondary sources are then turned upside down so that the microphones can measure the pressure on the whole sphere. The power estimation is then calculated from equation (6) assuming that the

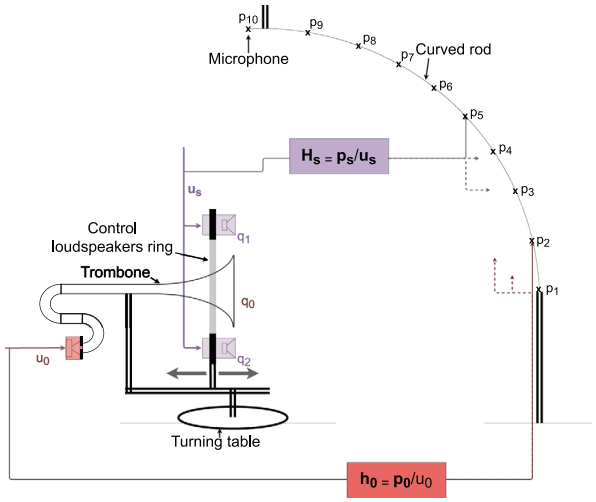

Figure 6. Simplified presentation of the experimental setup for a case with 2 secondary sources. Transfer functions $\boldsymbol{H_s}$ and $\boldsymbol{h_0}$ between voltages at sources and pressures at receivers are represented by boxes.

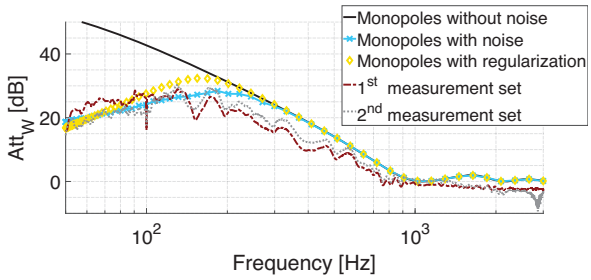

Figure 7. Power attenuation $\mathrm{Att_W}$ for case **3** (8 sources). Theory: $h_r = 0.16$ m without a random noise (solid line), with a random noise (solid line with crosses), or with regularization ($\beta = 200$, diamonds). Measurement (over 2 sets, dashed line and dotted one): 8 control speakers on a ring are placed at $h_r = 0.16$ m as shown in Figure 5.

turntable and the frame holding the sources (covered with absorbing foam) do not influence the acoustic radiation.

4.2 Power minimization

The power attenuation resulting from the far field control estimated in Section 2.2.2 is assessed experimentally. Figure 7 shows the power attenuation for a case with 8 control speakers on a ring at $h_r = 0.16$ m. It compares theoretical and experimental results obtained from two sets of measurement. First, experimental results are compared to the theoretical ones without adding an artificial noise or regularization. Secondly, the effect of artificial noise (without a regularization term) are presented. Experimental and theoretical results are then compared.

For 8 control speakers case, experiment fits with theory for frequencies higher than 500 Hz. Before, it drops off little by little with a difference of 6 dB at 200 Hz. The minimum attenuation is as expected at $kh = \pi$ ($f = 1$ kHz). The attenuation is negligible beyond that, with a slight increase in amplification up to 3 dB.

For frequencies lower than 200 Hz, the discrepancy between experimental and theoretical results increases as frequency decreases. This difference can be explained by several error sources: a weak signal to noise ratio (S/N), variation in the source-receiver distance, variation of temperature and presence of room modes.

First, the S/N has been measured at 37 dB around 100 Hz. The background noise is mainly electrical and decreases with frequency, leading to a greater impact at low frequencies. This weak S/N influences the matrix inversion (made with backslash on MATLAB). The conditioning number of $\boldsymbol{A_1}$ reaches effectively around 10^5 below 350 Hz and decreases to 10^2 in high frequencies. This high conditioning number justifies why the matrix inversion cannot allow to reach a power attenuation equivalent to the theoretical one. Moreover, it remains modes in the room up to 140 Hz. Some microphones may be located on nodes which induces a weak S/N also, and local variations of the resulting power attenuation below 200 Hz.

Secondly, the acoustic center of the trombone moves inside the trombone as the frequency increases [24]. In addition, when the secondary sources rotate over 360°, the distance between each receiver and each source varies. Moreover, the pressure measurement on all points around the sphere lasts at least 5 h. The temperature of the room varies during this time about 4 °C, leading to a variation of celerity. These three types of variation generate a phase error compared to the theory, estimated to 1.5°, which induces local variations of the power attenuation *versus* frequency.

These errors have been simulated by adding an artificial noise on the theoretical propagators $\boldsymbol{g_0}$ and $\boldsymbol{G_s}$ inducing a S/N of 34 dB at 100 Hz. It is chosen for the rest of the study that only noise is added to the theory to fit the measurement. This adding of an artificial noise allows to fit the theory with the experimental results for power attenuation (solid line with crosses in Fig. 7, solid line and solid one with crosses in Fig. 8, solid line and solid one with crosses in Fig. 9). Experimental attenuation can also be fitted by adding regularization in the matrix inversion ($\beta = 200$) without added noise (diamonds in Fig. 7).

When a ninth source is added at $h_f = 0.05$ m on the trombone main axis of radiation, the power attenuation is shown in Figure 8. Results show that the experimental attenuation (dash and dot lines) is greater than the theoretical one (solid line and solid one with crosses).

A deviation is still present at low frequencies up to 200 Hz which is similar to the previous case. Beyond 2 kHz, the attenuation is null, with a small increase in amplification up to 5 dB.

The attenuation estimated by the experimental model is greater than the theoretical one between 350 Hz and 2000 Hz. This gap can be explained by a modification of the field radiated by the primary source due to the position of the ninth secondary source close to the trombone bell ($h_f = 0.05$ m). Experiment seems to fit with theory up to 1500 Hz when the distance between the trombone and the speaker 9 is chosen equal to 0.0085 m in the theoretical

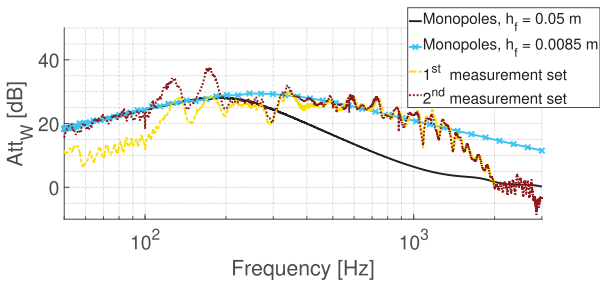

Figure 8. Power attenuation Att_W for case **5** (9 sources). Theory with a random noise: $h_r = 0.16$ m and $h_f = 0.05$ m (solid line) or $h_f = 0.0085$ m (solid line with crosses). Measurement (over 2 sets, dashed line and dotted one): 8 control speakers on a ring are placed at $h_r = 0.16$ m and a ninth one at $h_f = 0.05$ m front of the trombone.

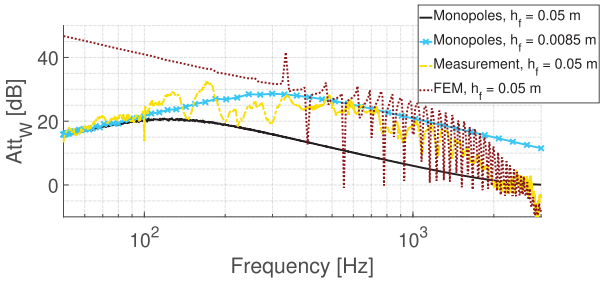

Figure 9. Power attenuation Att_W for case **1** (1 source). Theory with a random noise: $h_f = 0.05$ m (solid line) or $h_f = 0.0085$ m (solid line with crosses). Measurement (dashed line): $h_f = 0.05$ m with 1 control speaker placed in front of the trombone. FEM without added noise (dotted line): $h_f = 0.05$ m.

model (dashed & dotted line in Fig. 8). In that case and for frequencies below 1500 Hz, the control speaker acoustic center position would be located a few centimeters in front of its membrane as reported in [25, 26]. The effective distance between the trombone acoustic center and the ninth source acoustic center would be smaller than the physical one. This effect could explain the experimentally estimated over-attenuation and will require further study to confirm this hypothesis.

To verify this hypothesis, the power attenuation of a trombone with a single control speaker in front of the bell is studied. A 2D axisymmetric finite element method (FEM) model of the system is designed with COMSOL Multiphysics® and used to validate the experimental model and is shown in Figure 9.

A plane wave primary source with a volume velocity q_{in} is placed at the throat of the instrument. A secondary source of volume velocity q_{ss} is modeled as a piston mounted in a closed box. It can be considered as an omnidirectional source in the low frequency range. The source is placed at $h_f = 0.05$ m in front of the instrument. The diameter of its diaphragm is 3″, the diameter of its enclosure is 5″ and its length is 2″. Viscothermal losses at the wall surfaces are not taken into account. A perfectly matched layer at the edge of the domain mimics air surrounding the instrument as an open and non-reflecting infinite domain. As for the experimental protocol, the power attenuation is estimated on pressure points equally distributed around the source in far field with equation (6).

The power attenuation estimated by FEM fits quite well with the experimental one from 500 Hz to 3 kHz for a case with 1 source placed at $h_f = 0.05$ m. A difference can be observed at the peak and dip positions which is due to the absence of damping in the instrument's numerical model.

FEM and experience power attenuations do not fit with the analytical one. The secondary source has to be placed at 0.0085 m in the analytical model to fit with the FEM one. This would suggests that the primary and secondary equivalent sources come closer together when a secondary source is located in front of and close to the bell of the instrument.

4.3 Impact on the input impedance

The power attenuation for different setups having been investigated, it is now necessary to study the impact of the external control on the input impedance of the instrument. Previous results [13] showed that an external control has a very small impact on the three first impedance peaks of a cylindrical waveguide terminated with a bell – of the order of 1 dB on the amplitude and of the order of a ten of cents on the frequency. In this work, the secondary source impacting the most the input impedance should be the one placed closest to the bell of the trombone. The case **1** of Figure 2 where only one control speaker is placed at $h_f = 0.05$ m from the primary source is thus studied. The input impedance is not measured in the presence of control but is predicted from measurements of experimental transfer functions.

4.3.1 Experimental procedure

Figure 10 shows the experimental setup used for the input impedance prediction due to control. The primary source is mounted in an impedance sensor [27, 28] on a rear cavity with pressure p_{0_r} and leading to a resonator whose pressure in front of the impedance sensor is p_{0_f}.

The input impedance of the resonator is estimated from the measurements of $H_{0_f} = \frac{p_{0_f}}{u_0}$ and $H_{0_r} = \frac{p_{0_r}}{u_0}$ (respectively the front and the back sensor pressure response) by:

$$Z_i = \frac{p_{0_f}}{q_{0_r}} = \frac{H_{0_f}}{H_{q_{0_r}}}, \tag{16}$$

with $H_{q_{0_r}} = \frac{q_{0_r}}{u_0}$ the volume velocity response of the primary source rear part. From the calibration of the impedance sensor, it is possible to determine the relationship between $H_{q_{0_r}}$ and H_{0_r} by $H_{q_{0_r}} = f(H_{0_r})$. The impedance is thus written:

$$Z_i = \frac{H_{0_f}}{f(H_{0_r})}. \tag{17}$$

This formulation is given by the input impedance measurement system and is detailed in [27, 28]. Knowing that the

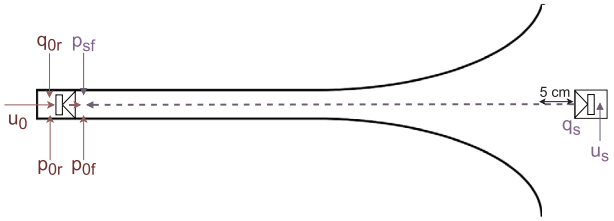

Figure 10. Simplified presentation of the experimental setup of a control with an impedance sensor attached to a 1 m plastic pipe connected to the trombone. One control speaker is placed at 0.05 m from the bell of the trombone.

secondary voltage is $u_s^{\text{opt}} = w_2 u_0$ $\left(w_2 = \frac{u_s^{\text{opt}}}{u_0}\right)$, the impedance with control is written:

$$Z_{ic} = Z_i\left(1 + \frac{H_{s_f}}{H_{0_f}} w_2\right), \tag{18}$$

with $H_{s_f} = \frac{p_{s_f}}{u_s}$ the pressure response of the secondary source at the front of the impedance sensor.

4.3.2 Results

The experimental impact of the acoustic power control on the input impedance is shown in Figure 11 when an impedance sensor attached to a 1 m plastic pipe is connected to the trombone as shown in Figure 5. The slide has been removed so the trombone position is not related to a particular note in the musical scale.

The input impedance amplitude deviation without and with control is defined for each peak from their real part. The frequency deviation is estimated when the imaginary parts cross 0 at the resonances. These deviations are given in dB for the amplitude and in cents for the frequency in Table 1.

When looking to the 10 first peaks of the trombone input impedance for a case with a loudspeaker placed at 0.05 m from the bell, the maximum frequency deviation is about 3 cents for the seventh peak and the amplitude shift reaches up to 6.6 dB for the ninth one. Globally, the power control impact on impedance is almost inexistent up to the fifth resonance of the trombone.

The higher impedance amplitude due to the control in high frequencies slightly makes the trombone easier to play as shown in [7]. This would have the impact of producing a different timbre at these frequencies. Nevertheless, the impact of the control for several positions of the trombone slide should be studied to validate these first results.

It can be assumed that the bell shape of the instrument as well as the ratio between the bell diameter and the control speaker membrane diameter (always smaller than that of the trombone bell in our case) reduces the influence of the radiating impedance on the input impedance of the trombone.

An active control external to the trombone therefore seems to have very little impact on the first peaks of the input impedance of the instrument, of the order of 3 cents

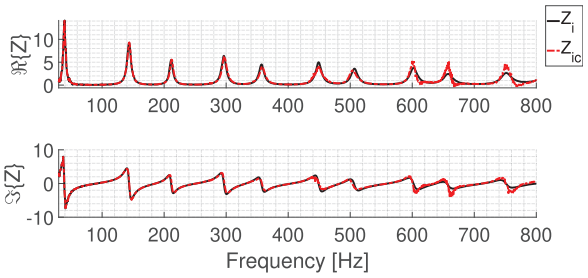

Figure 11. Experimental input impedance real and imaginary parts without control (Z_i – solid line) and with control (Z_{ic} – dashed line). Only one control speaker is placed at 0.05 m from the trombone's bell (case **1**).

of maximum frequency deviation and less than 2 dB of amplitude deviation for frequencies below 600 Hz, the effect on the musician's playing thus being very limited.

5 Practical feasibility

The aim of this section is to evaluate the required voltage to be applied to the secondary sources when the trombone is played by a musician and not excited by a loudspeaker. The volume velocity produced by the primary source is measured so that the electrical power to be applied to the control speakers and the maximum displacement of moving part can then be calculated – as developed in Section 2.2.3. The practical feasibility of the control is finally determined by the physical limits of the control speakers.

It is considered that the control system (ring of secondary sources + the one in front of the trombone) is not necessarily attached to the trombone. The weight of the control speaker is thus not studied in this work. In that case, the power attenuation efficiency would be reduced if the musician moves which is also not considered here.

5.1 Volume velocity measurement

The trombone volume velocity q_0 is estimated to evaluate the secondary source requirements. To do so, the source is considered as a monopole like illustrated in Figure 12.

Knowing that the trombone is omnidirectional at least until 500 Hz [15], the primary source volume velocity is estimated assuming a least square linear regression [29]. A measurement of the sound level radiated by the trombone according to the distance is set up in order to estimate the trombone volume velocity for several notes: 2 microphones are positioned in front of the pBone bell to estimate q_0 for 19 notes played by a trombonist. These notes played at a *fortissimo* input level wrap the set of notes that can usually be played by a trombonist (i.e. diatonic scale from F2 (f_0 = 87 Hz) to F4 (f_0 = 349 Hz), B♭1 (f_0 = 58 Hz), B♭2 (f_0 = 117 Hz), B♭3 (f_0 = 233 Hz) and B♭4 (f_0 = 466 Hz)). An example of trombone spectrum for the note B♭4 (f_0 = 466 Hz) is given in Figure 13. The pressure

Table 1. Amplitude (ΔA) and frequency (Δf) deviations for the first 10 peaks of the trombone input impedance without and with control for a case with a loudspeaker placed at 0.05 m from the bell (case **1**).

Peak no.	1	2	3	4	5	6	7	8	9	10
f (Hz)	39	143	211	297	357	450	505	602	659	752
ΔA (dB)	<0.1	0.1	0.2	0.1	0.9	1.7	0.8	2.9	6.6	4.8
Δf (cent)	<1	1.1	2.2	1.6	1.5	0.5	3.1	1.3	0.9	0.7

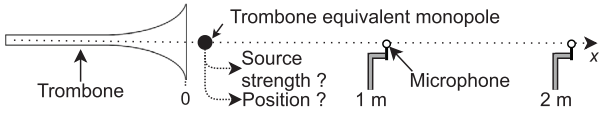

Figure 12. Diagram for the measurement of the volume velocity of the trombone, considered as a monopole. Its position and its volume velocity must be estimated as a function of frequency.

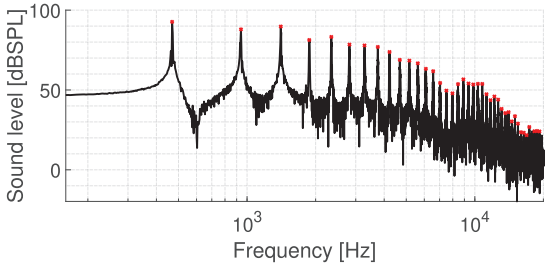

Figure 13. Spectrum for the note $B\flat 4$ ($f_0 = 466$ Hz) at 1 m with a *fortissimo* input level. Red dots are placed at each resonance peaks.

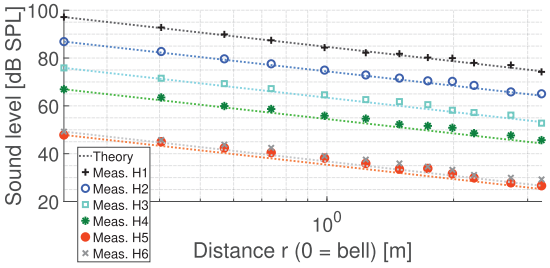

Figure 14. Measurement of the sound level decrease according to the distance for the six first harmonics H1 to H6 of the note $B\flat 4$ ($f_0 = 466$ Hz) with 12 microphones placed from 0.2 m to 3.5 m. Dotted lines represent the theoretical sound pressure level $L_p = L_{p0} - 20\log(r)$ with L_{p0} the sound pressure level at 0.2 m from the trombone.

peak value is measured for the first 40 harmonics of the note, containing most of the signal energy, to estimate q_0.

To endorse the measurement, the monopole pressure decrease presented by equation (5) is assessed by measuring the pressure decrease over 3.5 m in the measurement anechoic room with 12 microphones. Figure 14 shows the pressure decrease over distance for the six first harmonics of the note $B\flat 4$ ($f_0 = 466$ Hz).

The decrease of the sound level as a function of the distance shows some fluctuations: the nearest microphones are in the source nearfield. It is considered that the receivers must be positioned from at least $d = \frac{c}{2\pi f_{\min}} \simeq 0.36$ m (with $f_{\min} \simeq 150$ Hz the anechoic room cut-off frequency exceeding the lowest fundamental frequency of the trombone) to be in free field [30]. The 6 furthest microphones have a weak signal-to-noise ratio due to several reflections in the room and can therefore not be taken into account. These disturbances are due to the grid (causing vibrations, diffraction and reflections) used as a floor for the musician and allowing the set-up to be placed. Reflections and diffraction are also coming from the lamps placed near the ceiling. For the measurement, the microphones are then placed between 0.5 and 1 m from the source.

The measurement gives an accurate overview of the trombone behaviour for a high input level: the maximum volume velocity for a harmonic can reach about $q_0 \simeq 5 \times 0^{-3}$ m^3 s^{-1} as illustrated in Figure 15. The volume velocity amplitude spectrum is similar to a bell curve whose sound level can reach up to 110 dB SPL at 1 m.

The volume velocity estimation allows an evaluation of the electromechanical limits of the control loudspeakers as a function of the note and the sound level produced by the trombone.

5.2 Technological limits

The feasibility of an external active control using an electrodynamic loudspeaker is assessed from the experimental control results presented in Section 4 combined with the trombone's volume velocity measurement presented in Section 5.1.

The speaker volume velocity is defined according to its *T&S* parameters [31] and can thus be compared to that required for a control with a *fortissimo* primary source input level. The maximum displacement of the speaker diaphragm is also confronted to the required one. The used loudspeaker is a *Beyma 3FR30Nd* with a resonance frequency F_s of 188 Hz, a nominal power W_{nom} of 30 W, an input impedance Z_e of 6.4 Ω, an effective surface area S_d of 0.003 m^2 and a maximum excursion $x_{\max}$ of 4.5 mm.

5.2.1 Electrical power

Lets simulate for this part a control when the note $B\flat 4$ ($f_0 = 466$ Hz) – shown in Figure 13 – is played. This first setup includes 8 control speakers placed at $h_r = 0.16$ m from the primary source (case **3**). The corresponding power attenuation is displayed in Figure 7. The required electrical

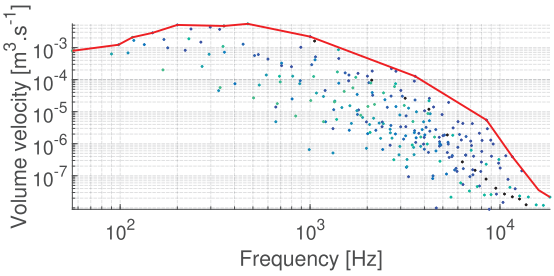

Figure 15. Trombone maximum volume velocity envelope (solid line) gathering 19-note harmonics (dots). The six dot colors correspond to the six first harmonics of each note.

input power for a control loudspeaker i depends of its optimal driving voltage $\boldsymbol{u}_{\mathbf{s}}^{\mathbf{opt}}$ developed in Section 2.2 and can be expressed as:

$$W_i = \frac{1}{Z_s} \sum_{\omega_j}^{N_\omega} |\mathbf{u_i^{opt}}(\omega_j)|^2, \tag{19}$$

with $\boldsymbol{u}_{\mathbf{i}}^{\mathbf{opt}} = \boldsymbol{w_3}\, q_0$ the optimal voltage for the speaker i as defined in Section 2.2.3, ω_j the pulsation of the resonance peaks central frequency, N_ω the number of pulsation points and Z_s the loudspeaker rated impedance.

Figure 16 confirms what Figure 4 shows: the required volume velocity (and so the needed voltage) for each speaker decreases as the frequency increases.

The input power is theoretically equally distributed if a power control system contains only equidistant secondary sources. In this work, the input power to be supplied to each loudspeaker can nevertheless be different because the measurements of the input voltages and transfer functions between sources and receivers imply variations between each secondary source during the experiment – due to electrical noise and the fact that the speaker positions are not exactly alike. For this example, the required power for each speaker placed on the ring W_r is about $W_r = 7.1 \pm 3.5$ W which does not exceed its power capacity W_nom.

If a control loudspeaker is added at $h_f = 0.05$ m ($8 + 1 = 9$ sources, Fig. 17), W_r is reduced to 0.3 ± 0.2 W but the required power for the speaker placed front of the trombone bell $W_f = 254$ W. The required power for W_f is higher than W_nom. For that case, it would be necessary to change this speaker with a more convenient one (for instance a *Morel EM 428* with a resonance frequency F_s of 68 Hz, a nominal power W_nom of 150 W and a maximum excursion x_max of 3.0 mm), or to add other speakers at the same distance to share the required input power, or to set an electrical limit to this speaker so that it does not distort. In the meantime, it is interesting to note that if a source is closer to the bell than the others, it strongly reduces the required power of the other sources while the needed power for this source increases strongly.

The very high input power of source 9 can be explained by the fact that its position is enough close to the primary source to experience the same problem as highlighted in Section 4.2 with Figure 8 where the power attenuation is bigger than the theory between 300 Hz to 2 kHz.

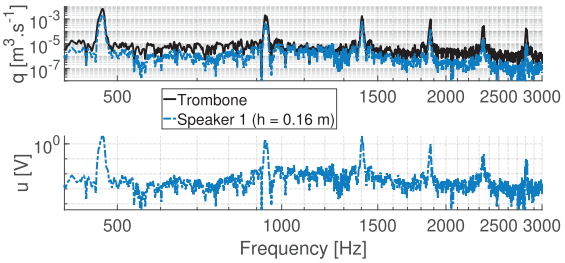

Figure 16. Volume velocity produced by the trombone and for one of the 8 speakers (top) and voltage of that latter (bottom) to control the note $B_\flat 4$ ($f_0 = 466$ Hz) – case **3** on Figure 2.

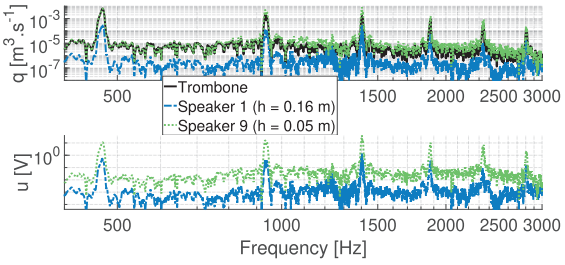

Figure 17. Volume velocity produced by the trombone and for the speakers 1 and 9 (top) and voltage of these latter (bottom) controlling the note $B_\flat 4$ ($f_0 = 466$ Hz) – case **5** on Figure 2.

5.2.2 Maximum excursion

Case **5** is used to observe the speakers maximum excursion. The volume velocity time signal is reconstructed from the optimal voltage spectrum calculated for each note, the required displacement spectrum being obtained from the following equation:

$$\boldsymbol{x}_\mathbf{s} = \frac{\boldsymbol{v}_\mathbf{s}}{j\omega}, \tag{20}$$

with $\boldsymbol{v_s} = \frac{\boldsymbol{q_s^{opt}}}{S_d}$. The needed displacement signal is then compared to the maximum displacement of the studied loudspeaker in Figure 18. The resulting required displacement is globally higher for the speaker 9 placed at $h_f = 0.05$ m front of the trombone which is nearer than the speakers 1–8 placed at $h_r = 0.16$ m on a ring. For cases where the fundamental frequency is low (below 300 Hz) and its energy is high (few cases above 130 Hz for these anechoic room measurements), the matrix inversion can require a higher volume velocity for the 8 speakers placed on a ring to control this fundamental, which requires a larger displacement than for speaker 9. It reaches a maximum of 2.5 mm for the speakers 1–8 and a maximum of 2.0 mm for the speaker 9. Both excursions always remain lower than the speaker's maximum displacement regardless of the note. Non-linearities nevertheless appear for such excursion.

Table 2 summarizes the cases studied in Figure 2 indicating the needed powers to be applied to the control loudspeakers as well as their maximum excursion to control the note $B_\flat 4$ ($f_0 = 466$ Hz).

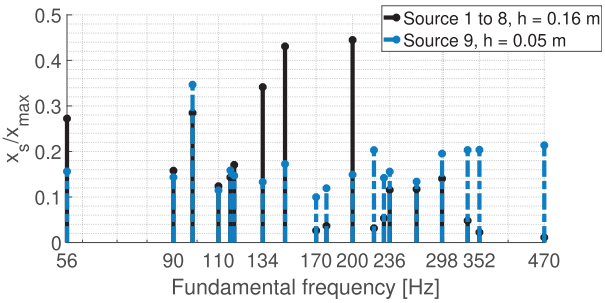

Figure 18. Excursion ratio $\frac{x_s}{x_{\max}}$ between the required excursion to control the note i and the speaker maximal excursion (speakers 1 and 9) for the case **5** in Figure 2.

Table 2. Power requirement for loudspeaker layer (Lay.) 1 and 2 and maximum required excursion $x_{s_{\max}}$ according to cases studied in Figure 2 to control the note B♭4 ($f_0 = 466$ Hz).

Case	N_s (Lay. 1 + 2)	W_i [W]		$x_{s_{\max}}$ [mm]
		Lay. 1	Lay. 2	
1	0 + 1	∅	268	1.0
2	3 + 0	23.7 ± 5	∅	0.8
3	8 + 0	7.1 ± 3.5	∅	0.4
4	3 + 1	0.5 ± 0.3	265	1.0
5	8 + 1	0.3 ± 0.2	249	1.1

For all the cases studied in Table 2, the input power to be applied to the control speakers is always the limiting factor, x_s never exceeding about $\frac{1}{2}$ of the speaker maximal excursion. A control is thus feasible using a minimum of three loudspeakers in that last example for a *fortissimo* primary source input level. As soon as several layers of speakers are used, a compromise must be found so that the input power of the speaker close to the primary source does not exceed its nominal power. The control system must then limit the input power of this speaker or add other sources to share the input power.

6 Conclusion

Results show that an active control placed outside the trombone is feasible and can be efficient up to 2000 Hz for the best case of study with a source close to the bell output ($h = 0.05$ m).

Several theoretical control strategies have shown that controlling with multiple layers of actuators (e.g. 8 speakers on a ring and a source closer to the instrument) allows to attenuate the power of the trombone more towards high frequencies.

In addition to the theory, the experiment showed that placing a secondary source very close to the primary source modifies the pressure field of the instrument in such a way that it is possible to obtain a power attenuation greater than that predicted by the analytical model which assumes that sources can be considered as monopoles. The modification of the equivalent acoustic center position of the sources due to their interaction is a possible way to explain this discrepancy.

Experimental studies on the input impedance of the instrument show that the playability of the instrument is very slightly affected by the control: the five first resonance peaks are not modified. This can be partly explained by the musical instrument's geometry, which limits the interaction of a secondary source – even one positioned very close to the bell – with the instrument's mouthpiece. A numerical model would provide a better understanding of the effect of the position and size of the secondary source relative to the primary source bell.

The electrical power to be applied at the input of the control loudspeakers is the limiting factor of the power control (and not the speaker maximum excursion). The secondary source closest to the primary source must provide the majority of the acoustic energy required for active control which can be difficult to achieve.

The external control set up allows to control the low frequency harmonics produced by the trombone. For future work, a passive mute which deals with the higher frequency range (from 1000 Hz), like foam placed at the bell of the trombone, could be added to complete the efficiency of this active control. A directivity control of the instrument would furthermore provide the possibility to direct the radiated sound of the instrument as desired, e.g. towards the musician. Finally, real-time control could be implemented using already existing technologies for such applications [32]. The first step would be to assess the control effectiveness by applying the optimal filters experimentally. A controller could then be used to perform a real time control (feedback or feedforward) when the instrument is played by an artificial mouth or a compression driver.

Conflict of interest

The authors declare no conflict of interest.

Acknowledgments

The authors would like to thank Joël Gilbert for being available many times to be recorded while performing trombone in order to characterize the instrument. They also want to thank Emmanuel Brasseur, Hervé Mézière, Éric Égon and Jacky Maroudaye for being involved in the setting up of the different experiments.

References

1. M. Campbell, J. Gilbert, M. Myers: The Science of Brass Instruments, Springer-Verlag. 2020, chapter 4.5.
2. A. Schneider: Studies in musical acoustics and psychoacoustics, Springer International Publishing. 2018, pp. 143–185.
3. J. Backus: Input impedance curves for the brass instruments. Journal of the Acoustical Society of America 60, 2 (1976) 470–480.

4. R. Caussé, B. Sluchin: Mutes of brass instruments – experiments and calculations. Journal of the Acoustical Society of America 71, S1 (1982) S91–S92.
5. S. Yoshikawa, Y. Nobara: Acoustical modeling of mutes for brass instruments, in: Studies in Musical Acoustics and Psychoacoustics, Springer, Cham. 2017, pp. 143–186.
6. L. Velut, C. Vergez, J. Gilbert: Physical modelling of trombone mutes, the pedal note issue. Acta Acustica United with Acustica 1034 (2017) 668–675.
7. T. Meurisse, A. Mamou-Mani, R. Caussé, B. Sluchin, D.B. Sharp: An active mute for the trombone. Journal of the Acoustical Society of America 138, 6 (2015) 3539–3548.
8. P. Pickett: An investigation of active tonal spectrum control as applied to the modern trumpet. Master Thesis, Blacksburg, VA, USA, 1998.
9. J. Guerard: Modélisation numérique et simulation expérimentale de systèmes acoustique. Application aux instruments de musique. PhD Thesis, Université Paris VI, 1998 (in French).
10. T. Meurisse, A. Mamou-Mani, R. Caussé, B. Chomette, D.B. Sharp: Simulations of modal active control applied to the self-sustained oscillations of the clarinet. Acta Acustica United with Acustica 100, 6 (2014) 1149–1161.
11. M. Jossic, A. Mamou-Mani, B. Chomette, D. Roze, F. Ollivier, C. Josserand: Modal active control of Chinese gongs, Journal of the Acoustical Society of America 141, 6 (2017) 4567–4578.
12. K. Buys, D. Sharp, R. Laney: Developing and evaluating a hybrid wind instrument. Acta Acustica United with Acustica 103, 5 (2017) 830–846.
13. C. Ayrault, T. Laurence, M. Melon, B. Gazengel: Effet d'un contrôle actif sur l'impédance de rayonnement d'un guide, in: 13th French Congress on Acoustics, Le Mans, France, 2016 (in French).
14. C. Ayrault, A. Bonnet, C. Corno, M. Melon, B. Gazengel: Étude d'une sourdine passive et active pour trompette simplifiée, in: 14th French Congress on Acoustics, Le Havre, France, 2018 (in French).
15. N. Eyring, T. Leishman, W. Strong: Tenor Trombone Directivity Animations, Faculty Publications, 1387, BYU ScholarsArchive. 2014.
16. P.A. Nelson, A.R.D. Curtis, S.J. Elliott, A.J. Bullmore: The minimum power output of free field point sources and the active control of sound. Journal of Sound and Vibration 116 (1987) 397–414.
17. P.A. Nelson, S.J. Elliott: Active Control of Sound. Academic Press, London. 1992, pp. 416–420.
18. R. Koehler: Intensity error sensing in the active control of free field sound radiation. PhD Thesis, Adelaide University, Australia. 2001.
19. C.H. Hansen, S.D. Snyder: Active control of noise and vibration. Chapman & Hall, Spon. 1997.
20. C. Deffayet, P.A. Nelson: Active control of low-frequency harmonic sound radiated by a finite panel. Journal of the Acoustical Society of America 84 (1988) 2192–2199.
21. J.S. Bolton, B.K. Gardner, T.A. Beauvilain: Sound cancellation by the use of secondary multipoles. Journal of the Acoustical Society of America 98, 4 (1995) 2343–2362.
22. P.A. Nelson, S.H. Yoon: Estimation of acoustic source strength by inverse methods: part I, conditioning of the inverse problem. Journal of Sound and Vibration 233, 4 (1999) 643–668.
23. S.H. Yoon, P.A. Nelson: Estimation of acoustic source strength by inverse methods: part II, experimental investigation of methods for choosing regularization parameters. Journal of Sound and Vibration 233, 4 (1999) 669–705.
24. P.L. Rendon, R. Velasco-Segura, C. Echeverria, D. Porta, A. Perez-Lopez, R.T. Vazquez-Turner, C. Stern: Using Schlieren imaging to estimate the geometry of a shock wave radiated by a trumpet bell. Journal of the Acoustical Society of America 144 (2018) EL310.
25. M.S. Ureda: The effects of acoustic center on array directivity, in: 104th Audio Eng. Soc. Convention, Amsterdam, Netherlands. 1998.
26. J. Chang, J. Jensen, F. Agerkvist: Shift of the acoustic center of a closed-box loudspeaker in a linear array: investigation using the beamforming technique. Journal of the Audio Engineering Society 63 (2015) 257–266.
27. J.-P. Dalmont: Acoustic impedance measurement, part I: a review, Journal of Sound and Vibration 243, 3 (2001) 427–439.
28. J.-P. Dalmont: Acoustic impedance measurement, part II: a new calibration method. Journal of Sound and Vibration 243, 3 (2001) 441–459.
29. C. Cavaillès, C. Ayrault, M. Melon, J. Gilbert, B. Gazengel: Loudspeakers optimisation for active control of trombone radiation, in: International Congress on Sound and Vibration, Montreal, Canada. 2019.
30. D. Keele: Anechoic chamber walls: Should they be resistive or reactive at low frequencies? Journal of the Audio Engineering Society 42 (1994) 454–466.
31. R.H. Small: Direct radiator loudspeaker system analysis. Journal of the Audio Engineering Society 20, 5 (1972) 383–395.
32. S. Haykin, B. Widrow (Eds.): Least-mean-square adaptive filters, Vol. 31, John Wiley & Sons. 2003.

Cite this article as: Cavaillès C. Gazengel B. Melon M. & Ayrault C. 2022. Study of the optimal active control of a trombone. Acta Acustica, **6**, 18.